ADHESION BETWEEN LIPOSOMES MEDIATED BY THE CHLOROPHYLL a/b LIGHT-HARVESTING COMPLEX ISOLATED FROM CHLOROPLAST MEMBRANES

ANNETTE McDONNEL and L. ANDREW STAEHELIN

From the Department of Molecular, Cellular, and Developmental Biology, University of Colorado, Boulder, Colorado 80309

ABSTRACT

A highly purified chlorophyll a/b light-harvesting complex (chl a/b LHC; chl a/b ratio 1.2) was obtained from Triton-solubilized chloroplast membranes of pea and barley according to the method of Burke et al. (1978, *Arch. Biochem. Biophys.* **187:** 252–263). Gel electrophoresis of the cation-precipitated chl a/b LHC from peas reveals the presence of four polypeptides in the 23- to 28-kdalton size range. Three of these peptides appear to be identical to those derived from re-electrophoresed CPII and CPII* bands. In freeze-fracture replicas, the cation-precipitated chl a/b LHC appears as a semicrystalline aggregate of membranous sheets containing closely spaced granules. Upon removal of the cations by dialysis, the aggregates break up into their constituent membranous sheets without changing their granular substructure. These membranous sheets can be resolubilized in 1.5% Triton X-100, and the chl a/b LHC particles then reconstituted into soybean lecithin liposomes. Freeze-fracture micrographs of the reconstituted chl a/b LHC vesicles suspended in a low salt medium reveal randomly dispersed ~80-Å particles on both concave and convex fracture faces as well as some crystalline particle arrays, presumably resulting from incompletely solubilized fragments of the membranous sheets. Based on the ~80-Å diameter of the particles, and on the assumption that one freeze-fracture particle represents the structural unit of one chl a/b LHC aggregate, a theoretical mol wt of ~200 kdalton has been calculated for the chl a/b LHC. Deep-etching and negative-staining techniques reveal that the chl a/b LHC particles are also exposed on the surface of the bilayer membranes.

Addition of ≥2 mM $MgCl_2$ or ≥60 mM NaCl to the reconstituted vesicles leads to their aggregation and, with divalent cations, to the formation of extensive membrane stacks. At the same time, the chl a/b LHC particles become clustered into the adhering membrane regions. Under these conditions the particles in adjacent membranes usually become precisely aligned. Evidence is presented to support the hypothesis that adhesion between the chl a/b LHC particles is mediated by hydrophobic interactions, and that the cations are needed to neutralize surface charges on the particles.

J. CELL BIOLOGY © The Rockefeller University Press · 0021-9525/80/01/0040/17 $1.00
Volume 84 January 1980 40–56

KEY WORDS chloroplast membrane · chl a/b light-harvesting complex · membrane adhesion · reconstituted liposomes · freeze-fracture

One of the most striking features of green algal and higher plant chloroplasts is the arrangement of the internal photosynthetic membranes (thylakoids) into highly organized stacks or grana which are interconnected by a system of unappressed stroma membranes. Numerous biochemical and structural studies have demonstrated not only that stacking is a membrane surface phenomenon but also that it affects the spatial distribution of virtually all thylakoid membrane components studied so far (1, 27, 5). Thus, fractionation studies have shown the stroma membranes to be enriched in photosystem I (PSI) activity and to have a low photosystem II (PSII) content, while the grana membranes possess both high PSI and PSII activities (5). On the other hand, the coupling factor seems to be exclusively associated with stroma membranes (27).

Freeze-fracture replicas reveal that the functional differentiation of thylakoids is matched by a nonrandom distribution of intramembrane particles between stacked and unstacked membrane regions (32). Nevertheless, the functional significance and the structural basis for the membrane-membrane interactions in the chloroplast are still a matter of speculation as is the nature of the "membrane adhesion factor" (33).

As first reported by Izawa and Good (23), the morphological organization of thylakoid membranes can be controlled by cations. When isolated thylakoids are suspended in a low salt medium the membrane stacks fall apart. Simultaneously, the intramembrane particles of the grana and stroma membrane regions become intermixed and randomized (29, 31). Addition of appropriate concentrations of mono- and divalent cations can partially reverse these effects (23, 28, 31). Cations also control the functional activity of many chloroplast components, and a number of feedback control loops seem to depend on the cation composition of the different membrane-limited chloroplast compartments (8).

Several lines of indirect evidence have implicated the chlorophyll a/b light-harvesting complex (chl a/b LHC) in the stacking process. For instance, in developing chloroplasts the appearance of cation-mediated membrane adhesion coincides with the insertion of the chl a/b LHC into the thylakoid membrane (4). These changes parallel the segregation of the >110-Å E-face intramembrane particles that contain the chl a/b LHC into the forming stacked regions (4). Brief digestion with pronase or trypsin of experimentally unstacked chloroplast membranes removes rather selectively a 1,000-dalton segment of the chl a/b LHC and at the same time increases dramatically the concentration of cations needed to mediate restacking of the membranes (13). Prochaska and Gross (30) have shown that cations bind to the chl a/b LHC in Triton X-100 subchloroplast particles, and it has further been demonstrated in a number of ways that cations affect the self association of the isolated chl a/b LHC (34, 7, 12).

In the present study we use a combination of biochemical and structural techniques to provide conclusive evidence for the hypothesis that the chl a/b LHC is indeed responsible for the cation-mediated membrane stacking of chloroplast membranes.

MATERIALS AND METHODS

Peas (*Pisum sativum* var Laxton progress No. 9) and barley (*Hordeum vulgare* var Bounty No. 309) were grown in vermiculite moistened with half-strength Hoagland solution under a 16-h photoperiod. The chl a/b LHC was isolated from leaves according to Bose et al. (11). The purified chl a/b LHC with a chlorophyll a/b ratio of ~1.2, was dialyzed against unbuffered 10 mM NaCl in the cold to lower the salt and sucrose concentration of the sample. The dialysed preparation with an approximate chlorophyll concentration of 4 mg/ml was stored in 50-μl aliquots at −70°C. For reconstitution experiments, 10 mM EDTA, 10 mM KCl, 1.5% Triton X-100 was used as the dialysis medium in place of the 10 mM NaCl.

Slab gel electrophoresis was carried out according to Laemmli (24) on 12.5% polyacrylamide gels, at 5°C with a constant current of 15 mA. Aliquots of the isolated chl a/b LHC were solubilized in one of the following buffers for 5 min at room temperature: (*a*) 0.0625 M Tris-HCl, pH. 6.8, 2% SDS, 5% mercaptoethanol; (*b*) 0.0625 M Tris-HCl, pH. 6.5, 0.2% SDS, 0.1% mercaptoethanol; or (*c*) 0.1 M Tris, 2% SDS, 2% mercaptoethanol, 0.5 M urea. Complete dissociation was also carried out by incubating the chl a/b LHC in sample buffer (*c*) at 37°C overnight. Molecular weight markers used were bovine serum albumin, carbonic anhydrase, soybean trypsin inhibitor, and lysozyme (Sigma Chemical Co., St. Louis, Mo.). After the tracking dye reached the bottom of the gel, the gels were stained and destained according to standard procedures. For re-electrophoresis of the pigment-protein complexes, gel-slices containing the pigmented bands were cut out with a razor blade before staining of the gel, transferred to a second gel, and re-electrophoresed without further treatment.

Brief digestion of the unstacked chloroplast membranes was carried out by incubating thylakoid membranes at a chlorophyll concentration of 0.5 mg/ml in 1 μg pronase/ml (Calbiochem-Behring Corp., American Hoechst Corp., San Diego, Calif.; grade B) in 50 mM Tricine, pH. 7.6 for 15 min at 21°C.

For the ultrastructural analysis of the chl a/b LHC, the chl a/b LHC isolated from peas was used exclusively. For the prepa-

ration of the lipid vesicles the procedure of Gerritsen et al. (17) was followed with several modifications. Lecithin (soybean, ICN Nutritional Biochemicals, Cleveland, Ohio) was dissolved in chloroform, and the suspension was evaporated to dryness with N_2. The dried lipids were taken up in ice-cold 18 mM sodium phosphate, pH. 8, to give a lipid concentration of 10 mg/ml, and the suspension was sonicated for 1 min in a cleaning bath sonicator. To this preparation an equal volume of solubilized chl a/b LHC ([chl] = 3 mg/ml) from peas in 10 mM EDTA, 10 mM KCl, and 1.5% Triton X-100 was added with stirring, and the lipid protein mixture was subjected to three cycles of rapid freezing and thawing with liquid N_2. In control experiments the protein was omitted and instead phosphate buffer with 1.5% Triton X-100 was added. The preparation was then allowed to stand for 1.5 h at room temperature with gentle stirring before Biobeads SM-2 (Bio-Rad Laboratories, Richmond, Calif.) were added for 45 min at room temperature. After removal of the beads the mixture was freeze-thawed three more times and briefly (5–10 s) sonicated. In experiments designed to test the effect of cations, $MgCl_2$ or NaCl was added to aliquots of this preparation to give final concentrations of 2, 4, 6, 8, and 10 mM $MgCl_2$ or 40, 60, 80, 100, 120, and 140 mM NaCl, and the samples were allowed to stand at least another 0.5–1 h at room temperature.

This procedure resulted in a population of mostly single-walled small vesicles as well as some larger, multilamellar membrane sheets.

Freeze-fracturing and Freeze-etching

Samples for freeze-fracture studies were suspended in glycerol to give a final concentration of 33% glycerol, keeping the desired cation concentration constant, and frozen in liquid Freon-12. For freeze-etching, the salt concentration was lowered to <5 mM sodium phosphate. Replicas were prepared according to standard procedures on a Balzers BA360 freeze-fracture apparatus (Balzers Corp., Nashua, N.H.). Specimens were fractured at −108°C.; freeze-etching was carried out at −106°C. for 5 min. The replicas were examined in a JEOL 100C electron microscope.

Negative Staining

Samples for negative staining were spread on Formvar-coated grids and stained for 0.5 min with 0.5% aqueous uranyl acetate.

Optical Diffraction

Optical diffraction patterns were made with a Spectra Physics model 120 5 mW He-Ne Laser (Spectra-Physics Inc., Mountain View, Calif.) from negatives taken at × 50,000, and recorded with a lens-less Nikon camera. The diffraction patterns were measured on the film with a × 7 objective lens equipped with a micrometer grating, and the true spacings were calculated.

RESULTS

Gel Electrophoresis of the Isolated chl a/b LHC

To examine the biochemical composition of the pea and barley chl a/b LHC preparations and to ensure the purity of the complex before reconstitution studies, aliquots of all preparations of the isolated chl a/b LHC (chl a/b ratio = 1.2) were electrophoresed on polyacrylamide gels. After mild solubilization (5 min at room temperature in any one of the three sample buffers), typically two chlorophyll-protein (CP) complexes, CPII* (apparent mol wt ~80 kdaltons) and CPII (apparent mol wt ~30 kdaltons) with chlorophyll a:b ratios similar to the original sample, can be resolved in unstained gels of both barley and pea (Fig. 1, slots *a* and *c*). Occasionally, and under conditions that we have not been able to reproduce consistently, the broad pigmented band of CPII appears as two closely migrating bands. After staining with Coomassie brilliant blue three additional polypeptides (in the 23- to 28 kdalton range) appear on the gels

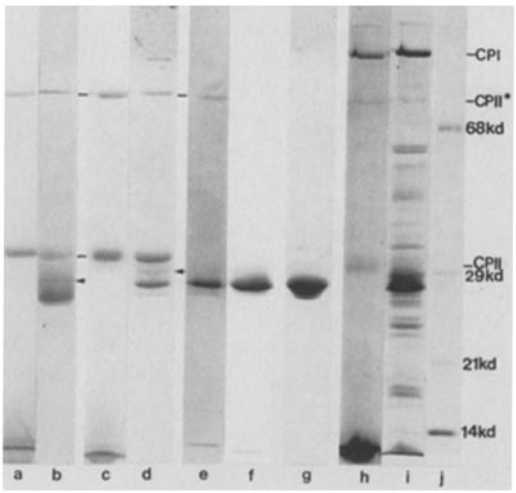

FIGURE 1 Gel electrophoresis patterns of the isolated chl a/b LHC from barley and peas. Samples were solubilized in sample buffer a (slots *a-f*) for 5 min at room temperature, and electrophoresis was carried out at 5°C on a 12.5% slab gel. Slot *g* shows the polypeptide pattern of a chl a/b LHC sample incubated in sample buffer c at 37°C overnight. Slots *a* and *c* are unstained gels, revealing the position of chl-protein complexes derived from barley (*a*) and pea (*c*) chl a/b LHC preparations. Slots *b* and *d* depict corresponding polypeptide patterns as revealed by Coomassie blue staining. The faint band marked by an arrow in slots *b* and *d* is probably a contaminating peptide, since it is absent in the re-electrophoresis pattern of the chlorophyll-protein complexes from peas, shown in slots *e* (CPII*) and *f* (CPII). For comparison, the unstained and stained gel electrophoresis patterns of whole thylakoids from peas are also shown (slots *h* and *i*). The position of the molecular weight marker proteins, bovine serum albumin (68 kdaltons), carbonic anhydrase (29 kdaltons), soybean trypsin inhibitor (21 kdaltons), and lysozyme (14 kdaltons), shown in slot *j*, are indicated at the right.

of the barley chl a/b LHC (Fig. 1, slot *b*) and four on the gels of the chl a/b LHC from peas (Fig. 1, slot *d*). The unexpected finding of a chlorophyll protein, CPII*, with an apparent mol wt of ~80 kdaltons, in the chl a/b LHC samples led us to examine this complex in peas in more detail. Slots *e* and *f* in Fig. 1 compare the polypeptide patterns of the eluted CPII* and CPII bands of pea chl a/b LHC samples after re-electrophoresis. The gels show that CPII* can give rise to traces of CPII as well as the same three nonpigmented bands (mol wt 23–25 kdaltons) that appear after re-electrophoresis of CPII and that are already present in the original chl a/b LHC sample. This finding is consistent with the hypothesis that CPII* is most likely the natural complex, i.e., comparable to the Triton-solubilized chl a/b LHC of the membrane, and that CPII and the three peptides appearing in the re-electrophoresis pattern are dissociation products of the complex. The fourth weak band (indicated by an arrow in slots *b* and *d*) is absent in the re-electrophoresis patterns of CPII* and CPII and therefore probably does not represent a genuine component of the chl a/b LHC, but is a peptide that copurified with our Triton-solubilized preparations of the chl a/b LHC. We also tested the effect of different solubilization buffers on the stability of the chlorophyll proteins, and found that with increasing concentrations of SDS and/or the addition of urea the greater the amount of dissociation of the CPII* complex and CPII.

This is most obvious in the sample incubated at 37°C. overnight in a buffer containing 2% SDS and 0.5 M urea, where a complete dissociation of CPII* and CPII into three polypeptides has occurred (Fig. 1, slot *g*). However, when even harsher solubilization conditions, such as boiling in SDS or extraction of the chl a/b LHC samples with 90% acetone were used, unspecific aggregation of the peptides seemed to occur as evidenced by the appearance of several new high molecular weight bands and streaking in the gels (not shown). As judged by the intensity of the Coomassie brilliant blue staining, the ratios of the three chl a/b LHC related peptides appeared to vary slightly from one chl a/b LHC samples to another (results not shown). For comparison, unstained and stained electrophoresis patterns of whole thylakoid membranes from peas are shown in slots *h* and *i*. In addition to the polypeptides, pigments and lipids were also present in all of our chl a/b LHC preparations.

Ultrastructural Characterization of the Isolated chl a/b LHC

Figs. 2 and 3 show freeze-fracture micrographs of the crystalline aggregates of the Triton-solubilized chl a/b LHC, precipitated out of solution with 10 mM $MgCl_2$ and 100 mM KCl. The precipitated material appears as tightly adhering layers of the chl a/b LHC particles with lenslike inclusions of the surrounding medium (Fig. 2). When fractured along the membranous sheets, the chl a/b LHC particles appear organized in the form of paracrystalline arrays with a center-to-center spacing of particles of ~118 Å (Fig. 3). After dialysis against 10 mM NaCl the membranous sheets of the crystalline aggregates become separated while maintaining essentially the same distribution of their constituent particles on their fracture faces (Fig. 4). Addition of 10 mM $MgCl_2$ to the dialysed samples leads to restacking of the membranous sheets into crystalline aggregates that are undistinguishable from those shown in Fig. 2. After solubilization by dialysis against Triton X-100, the membranous sheets break up into small fragments and into several individual granules. When chloroplast membranes were briefly treated with pronase just before the Triton solubilization step of the chl a/b LHC isolation procedure, a highly fluorescent band enriched in chl a/b LHC was obtained on the sucrose gradient as in the controls, but this chl a/b LHC could no longer be precipitated out of solution with the usual concentration of cations. However, precipitation might be possible with >15-mM concentration of Mg^{++} since Carter and Staehelin (13) have recently found that restacking of trypsin- or pronase-treated chloroplast membrane could be achieved by increasing the Mg concentration from 5 to 15 mM. This finding suggests that a cation-binding site on the stroma side of the membrane-bound chl a/b LHC is responsible for the precipitation reaction.

Ultrastructural Characterization of the Reconstituted Membranes

Fig. 5 is a freeze-fracture micrograph of pure lipid vesicles, prepared without the addition of the chl a/b LHC and showing completely smooth fracture faces. In contrast, vesicles reconstituted with the chl a/b LHC and suspended in a low salt (<10 mM sodium phosphate) medium exhibit numerous randomly distributed particles with a diameter of 80 Å (Fig. 6). The fact that particles are

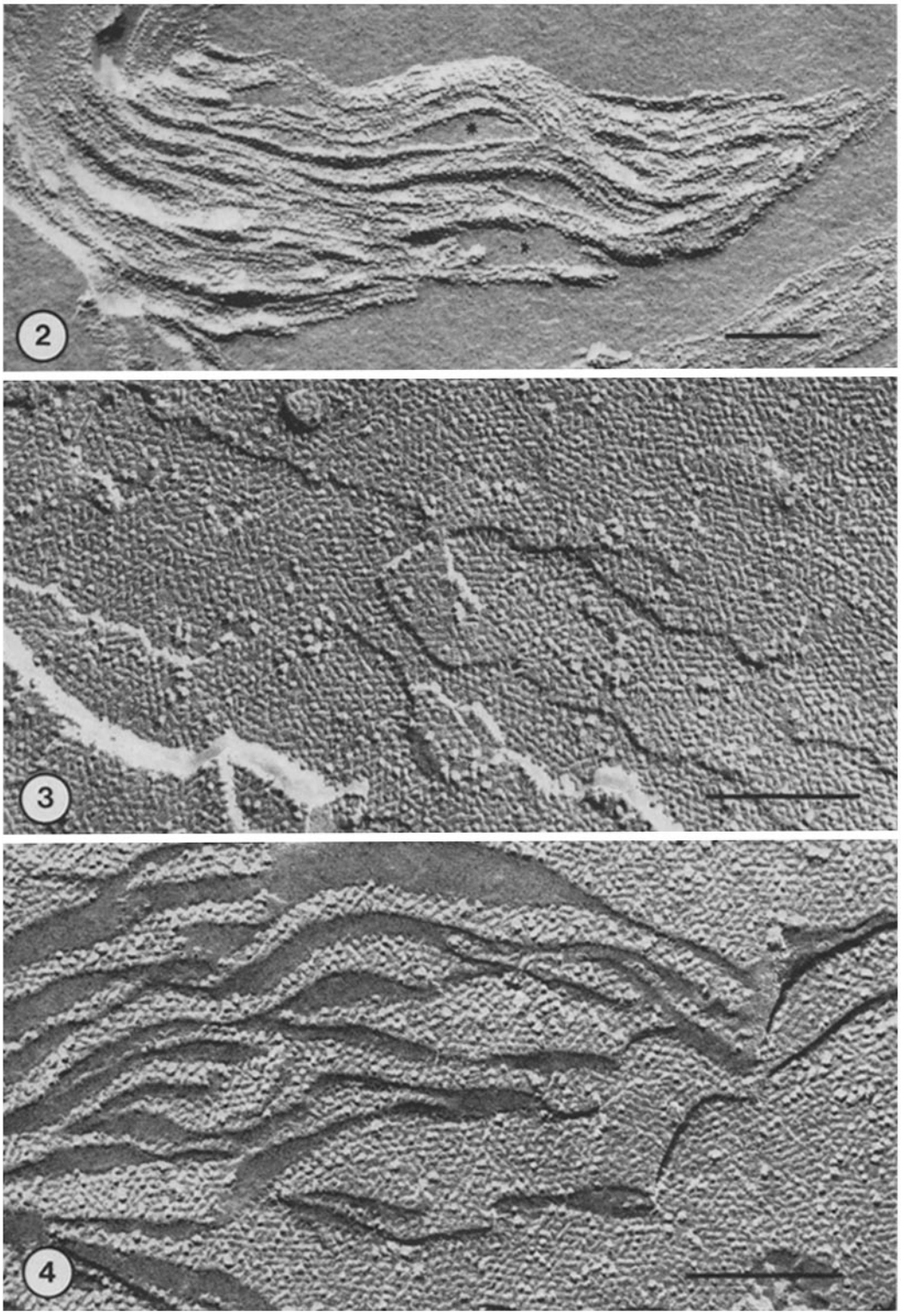
2
3
4

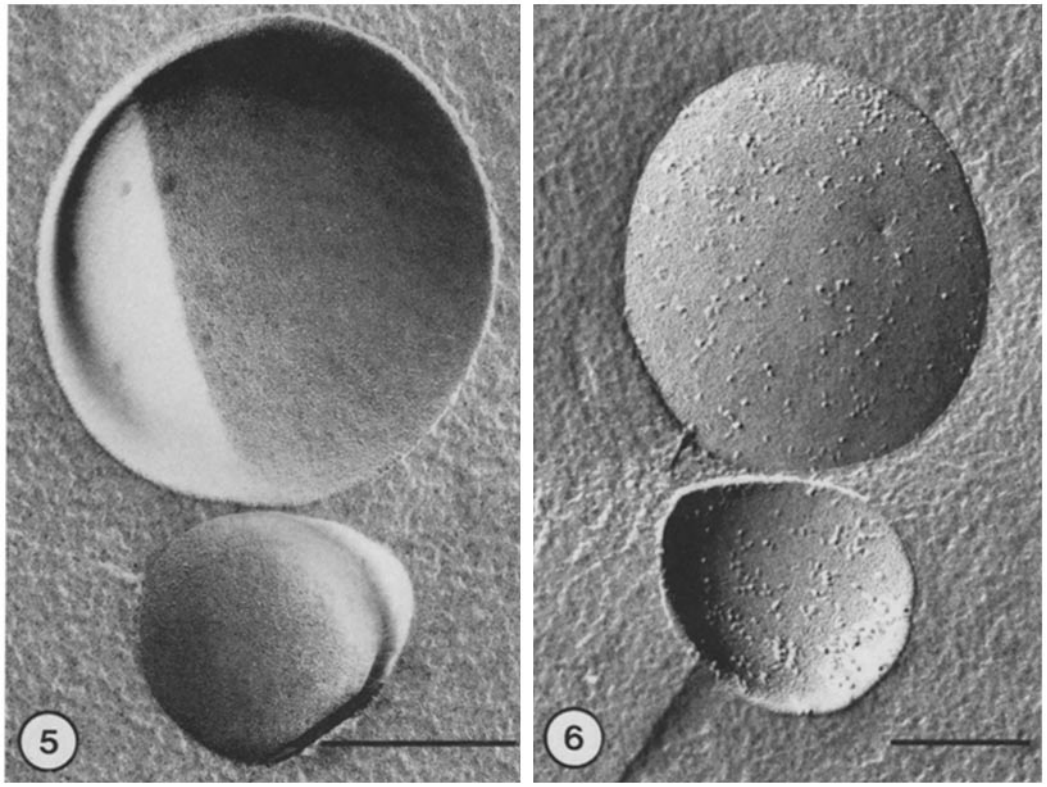

FIGURE 5 Lipid vesicles prepared without the addition of the chl a/b LHC and incubated in 4 mM $MgCl_2$ for 1 h at room temperature. Note the complete absence of intramembrane particles and the lack of vesicle adhesion. × 131,000.

FIGURE 6 Freeze-fracture micrograph of reconstituted lipid vesicles. Randomly distributed intramembrane particles, corresponding to the chl a/b LHC, are visible on both concave and convex fracture faces. × 92,000.

observed both on concave and on convex fracture faces suggests that the chl a/b LHC is randomly inserted into the lipid bilayers and is not uniformly oriented with respect to the outer surface of the vesicles. Fig. 7 demonstrates another feature of some of our reconstituted membranes, the occurrence of patches of densely packed and highly ordered intramembrane particles besides the randomly distributed ones. These arrays probably arise when fragments of incompletely dissociated

FIGURE 2 Freeze-fracture micrograph of the Triton-solubilized chl a/b LHC precipitated out of solution with 10 mM $MgCl_2$ and 100 mM KCl. The semicrystalline precipitate appears to consist of stacks of tightly packed membranous sheets with lenslike inclusions of the surrounding medium (*). Bar, 0.2 μm in this and subsequent micrographs. × 72,000.

FIGURE 3 A face view of the membranous sheets shown in Fig. 2. Tightly packed particles in paracrystalline arrays constitute these sheetlike structures. × 120,000.

FIGURE 4 Triton-chl a/b LHC precipitated out of solution as in Figs. 2 and 3 and then dialysed against 10 mM NaCl. Although the membranous sheets are clearly separated from each other, the paracrystalline distribution of the chl a/b LHC particles within the plane of each sheet appears the same as in the stacked, high-salt samples (cf. Fig. 3). × 120,000.

membranous sheets of the dialysed chl a/b LHC become incorporated into the lipid vesicles. This interpretation is supported by the finding that the number of arrays on the reconstituted membranes goes down when the Triton X-100 concentration is increased from 0.5 to 1.5% before reconstitution. As in the case for the randomly distributed particles, the particles within the arrays also seem randomly inserted as evidenced by the fact that we find numerous pits in the arrays but never pure arrays of pits. To demonstrate that the particles seen on the membrane fracture faces were also exposed on the membrane surface, we examined the true surfaces of the reconstituted membranes by deep-etching and negative staining techniques (Figs. 8 and 9). Although the resolution of our freeze-etch micrographs is insufficient to positively identify protruding elements of individual, randomly distributed particles, a clear particle-dependent substructure of the membrane surface can be detected where they are organized into geometrical arrays (Fig. 8). A similar substructure is evident in negatively stained images of the reconstituted membranes (Fig. 9). The following observations indicate that the hexagonal surface lattices are formed by, and are a different view of, the same particles that are seen in arrays on the fractured faces: Where an array of particles is seen on a fracture face lying immediately adjacent to an etched membrane surface region, the array zone appears continuous with the surface lattice zone across the ridge separating the two planes. The dimensions of the lattice as determined by optical diffraction on the fracture faces (80.3 × 84.3 × 87.3 Å) and on the etched surfaces (79.1 × 85.6 × 85.8 Å) and negatively stained preparations (81.6 × 84.3 × 84.3 Å) are very similar (cf. *insets* in Figs. 15, 8, and 9).

Effect of Cations on Vesicle Aggregation

Samples of the chl a/b LHC-containing vesicles placed in the wells of a microtiter plate and incubated in a series of monovalent and divalent cation concentrations revealed that vesicle aggregation occurred at salt concentrations of ≥2 mM $MgCl_2$ and ≥60 mM NaCl (Fig. 10). These salt concentrations are nearly identical to the cation requirement for restacking of experimentally unstacked chloroplast membranes (31, 33). This effect is specifically attributable to the chl a/b LHC since vesicles lacking the chl a/b LHC do not aggregate (cf. Fig. 5).

Ultrastructural Analysis of the Cation Effect

To examine the ultrastructural changes associated with the cation-mediated adhesion of the reconstituted chl a/b LHC vesicles, freeze-fracture specimens were prepared of samples allowed to equilibrate for 45 min at room temperature in solutions containing different amounts of monovalent and divalent cations. As seen in Fig. 6, no adhesion of the reconstituted vesicles occurs in the absence of any cations. Upon addition of 2 mM $MgCl_2$, however, limited areas of membrane contact become established (Fig. 11). When the Mg^{++} concentration is increased to 4 mM, these contact regions increase in area and begin to form small stacks (Fig. 12). At the same time, nearly all intramembrane particles become concentrated into the stacked membrane regions. Raising the Mg^{++} concentration to 10 mM produces even tighter and larger membrane stacks (Fig. 13). The particle-free blebs around the margins of the stacks suggest that the packing is so tight that the excess lipids are laterally displaced out of the stacked regions. Face views of stacked membranes reveal

FIGURE 7 Reconstituted chl a/b LHC membranes showing numerous randomly distributed particles besides particles organized into a geometric array. These arrays persist in the absence of membrane adhesion and they most likely represent remnants of incompletely dissociated sheets of chl a/b LHC particles from the salt-precipitated, dialysed pseudocrystals (cf. Fig. 4). × 117,000.

FIGURE 8 Freeze-etch image of a reconstituted vesicle revealing its true membrane surface. A hexagonally arrayed region on the membrane surface corresponding to a hexagonal patch of intramembrane particles seen in Fig. 7 is clearly visible. Ice (*I*); fracture face (*F*); × 124,000. *Inset:* Optical diffraction pattern of the arrayed surface region.

FIGURE 9 Negatively stained chl a/b LHC-containing membranes. A hexagonal substructure on the membrane surface is barely distinguishable. × 116,000. *Inset:* Optical diffraction pattern.


7


I
F
8

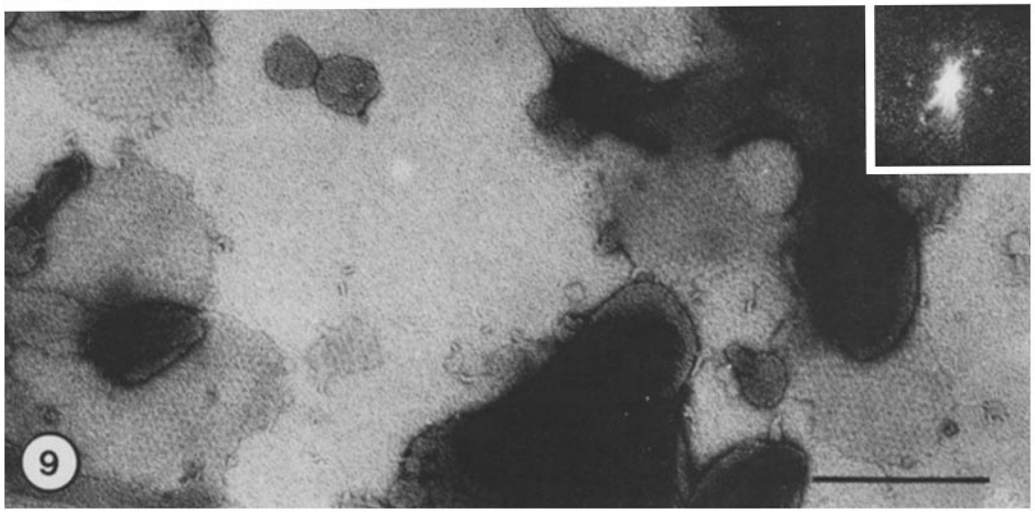
9

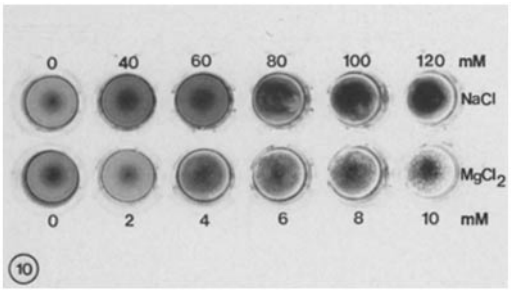

FIGURE 10 Microtiterplate illustrating the effect of cations on the aggregation of the reconstituted vesicles. 0–120 mM NaCl (upper row) or 0–10 mM $MgCl_2$ was added to the vesicle suspension, and the samples were allowed to stand overnight in the cold. Note the distinct aggregation of the reconstituted vesicles treated with ≥60 mM NaCl or ≥2 mM $MgCl_2$.

the intramembrane particles clustered into large hexagonal arrays which are often precisely aligned in adjacent membranes (Fig. 14). This precise alignment of the particles is consistent with the idea that the adhesion is mediated by particle-particle interactions.

Further quantitative studies of the effects of cations on the reconstituted chl a/b LHC membranes have revealed that, while the amount of stacking and the number of particles in hexagonal arrays goes up with higher concentrations of cations, the spacing of the particles within the hexagonal lattices remains virtually unchanged in both stacked and unstacked regions. The only exception was found in the 2- to 4-mM $MgCl_2$ samples which exhibited, in addition to the regular hexagonal arrays and continuous with them, arrayed regions with a slightly different geometrical organization (Fig. 15), resulting in a new and very distinct peak in the diffraction intensity with a spacing of ~120 Å along one axis of the hexagonal array (right *inset* in Fig. 15). In the freeze-fracture image this new pattern is reflected in a change in the packing of the intramembrane particles from the regular hexagonal array into a pattern of rows of particles, separated by grooves. In places, the dominant particle ridges appear to be formed by a "braided" double row of particles (Fig. 15, arrow).

Very similar results with respect to membrane adhesion are obtained with monovalent cations. Thus, when reconstituted vesicles are incubated in 60 mM NaCl a rather limited extent of membrane-membrane interaction can be seen, and although segregation of some of these particles into areas of membrane contact occurs, most of the particles remain still randomly distributed or clustered into small arrays in nonadhering membrane areas (results not shown).

Upon addition of ≥100 mM NaCl, however, the aggregation of particles into regions of membrane adhesion becomes very evident (Figs. 16 and 17), contrasting sharply to the random particle distribution of nonadhering membranes, and providing further evidence that the chl a/b LHC in adjacent membranes is indeed responsible for membrane adhesion. As shown in Fig. 17, a small, but noticeable change in the organization of the chl a/b LHC particles in the membrane may occur in regions of actual membrane contact (arrows).

Although both cations tested promote adhesion of the reconstituted membranes, we have observed quantitative and structural differences between the effect of divalent cations and the effect of univalent cations. Thus, when the reconstituted vesicles are incubated with ≥4 mM $MgCl_2$, the adhering vesicles tend to collapse, forming multilayered membrane stacks with virtually all particles concentrated in the adhering membrane regions. In samples incubated with ≥100 mM NaCl, on the other hand, multilayered stacks are seen far less frequently, the areas of membrane contact are less extensive, and even at high concentrations of NaCl a sizeable number (~20%) of the particles stay randomly distributed in the unstacked regions.

Fig. 18 provides yet another type of view of an adhering membrane region. In this case, the fracture plane appears to have developed over a small distance along the true membrane surface, presumably due to the high density of hydrophobic adhesion sites between the two membranes. Within this region the protruding chl a/b LHC particles resemble small, closely packed cylinders, whose flat tops are marked by a central depression. The uniformity of the particles in this membrane surface fracture is contrasted by the appearance of the particles on a regular type of fracture face (cf. Figs. 6, 7, 15–17) where they appear variable in both size and shape. This is consistent with the idea that, during normal membrane splitting, the randomly inserted chl a/b LHC particles could be plastically deformed and/or torn apart.

DISCUSSION

Ultrastructural Analysis of the chl a/b LHC in the Reconstituted Membranes

In our freeze-fracture electron micorgraphs of

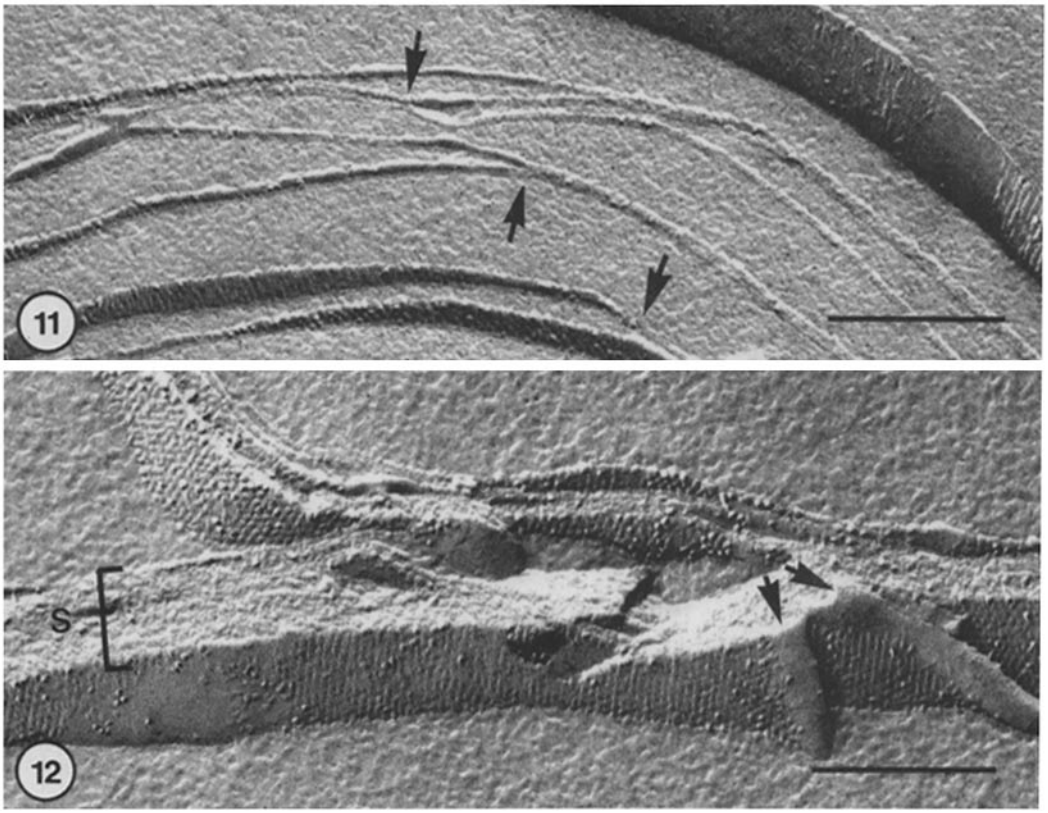

FIGURE 11 Cross-fractured, reconstituted membranes treated with 2 mM $MgCl_2$. Under these conditions the membranes appear loosely packed with limited areas of membrane contact (arrows). The intramembrane particles are either randomly distributed or packed into arrays with no clear correlation with regions of membrane contact. × 118,000.

FIGURE 12 Same sample as in Fig. 11, but treated with 4 mM $MgCl_2$. Most of the membrane sheets are organized into membrane stacks (*S*), with the intramembrane particles limited mainly to areas of membrane contact. Note the particle-free lipid blebs (arrows) around the margins of the stacks (see also Fig. 13). × 123,000.

reconstituted membranes, we have determined the size of the intramembrane chl a/b LHC particles as being 75–85 Å in diameter. Using ultrafiltration techniques, Arntzen and Ditto (6) estimated the digitonin-solubilized chl a/b LHC particles to have a diameter of 50–100 Å. A value of 50–80 Å has been reported by Burke et al. (12) based on thin-section images of crystalline aggregates of salt-precipitated Triton-derived chl a/b LHC. Based on these three measurements, it seems not unreasonable to assume that the actual diameter of the chl a/b LHC particles is ~80 Å. In 1977, Armond et al. (4) reported that, during greening of pea plants grown under an intermittent light regime, the insertion of the chl a/b LHC into the chloroplast membrane is paralleled by an increase in E-face particle size and the formation of grana stacks. Further analysis of the size changes revealed a step-wise growth of the particles, the growth increment per step corresponding to an increase in E-face particle volume of ~220,000 $Å^3$. The authors interpreted their data to indicate that the increase in volume of the E-face particles was due to the addition of 1, 2, or 4 chl a/b LHC aggregates to a PSII core particle already in the membrane. If the chl a/b LHC had a roughly spherical shape, then the volume of 220,000 $Å^3$ would correspond to a sphere with a diameter of ~75 Å. This value is sufficiently close to the size of 80 Å for the isolated chl a/b LHC particles used

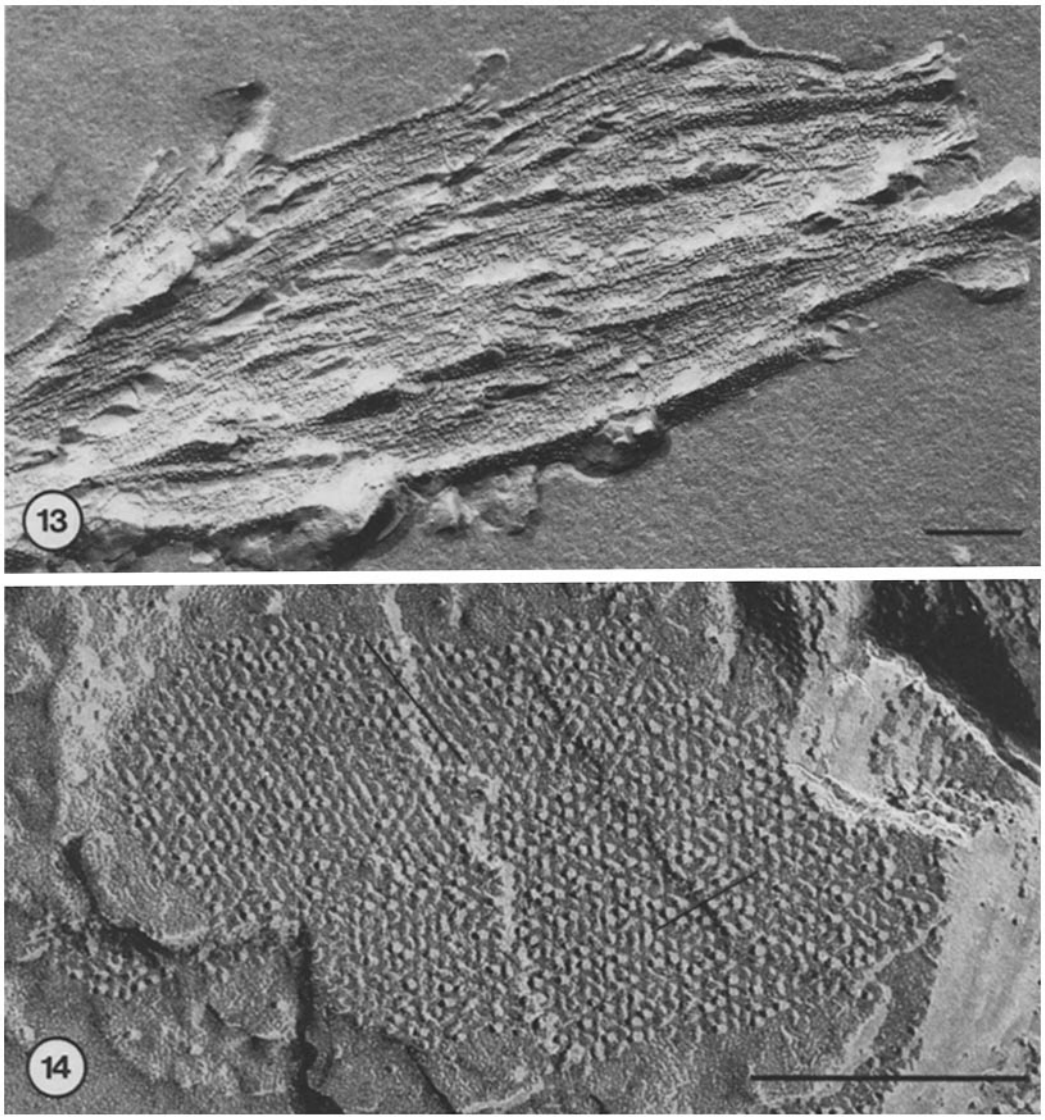

FIGURE 13 Reconstituted membranes in the presence of 10 mM $MgCl_2$. The particles in the stacked membrane regions are so tightly packed that the excess lipids appear to have been squeezed out of the stacks and into multilamellar blebs around the margins. × 65,000.

FIGURE 14 A face view of the membrane sample shown in Fig. 13. Note the alignment of the two different particle arrays (indicated by lines) over the appressed membranes, suggesting particle-particle interaction in areas of membrane contact. × 184,000.

in the present reconstitution studies to conclude that the chl a/b LHC particles as they appear in the reconstituted membranes could correspond to the natural chl a/b LHC aggregates that associate with the 80 Å PSII core elements in chloroplast thylakoids. We have used this structural information on the size of the chl a/b LHC particle to deduce its molecular weight, since it has been shown repeatedly (15) that molecular weight determinations using SDS gel electrophoresis are unreliable for chlorophyll proteins. Using relatively low and relatively high values of 1.25 g/ml

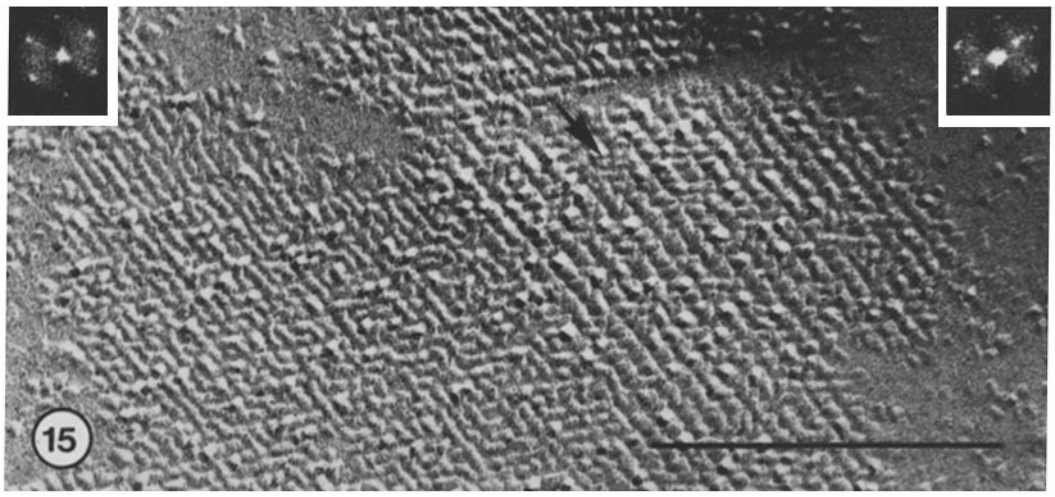

FIGURE 15 Freeze-fracture micrograph of a reconstituted vesicle incubated in 2 mM $MgCl_2$. A transition in the packing of the intramembrane particles from a regular hexagonal type to a slightly different pattern (right half of the micrograph) is clearly evident. The arrow points to a region in the dominant particle ridges, where a substructure can be distinguished. × 208,000. The left and right *insets* are optical diffractions of the respective areas. Note the additional strong diffraction spots in the right diffractogram.

to 1.45 g/ml for membrane protein density, we can calculate, according to the formula of Green and Fleischer (18), that an 80-Å chl a/b LHC particle should have a mol wt of between 202,000 and 234,000 daltons.

Role of the chl a/b LHC in Membrane Adhesion

As pointed out in the Introduction, several lines of indirect evidence support the hypothesis that the chl a/b LHC mediates membrane stacking in chloroplasts (5), but direct evidence has been lacking. By investigating the adhesive properties of the isolated and purified complex in reconstituted lipid membranes, we provide direct proof that the chl a/b LHC is the "adhesion factor" of chloroplast membranes. To this end it seemed important to show that the reconstituted membranes met the following criteria: The chl a/b LHC incorporated into the artificial membranes should be recognizable as a distinct particle on the fracture faces and should also be exposed on the membrane surface. The cation concentration needed to induce "stacking" of the reconstituted vesicles should be similar to the concentrations required for stacking of chloroplast membranes. And should adhesion between the reconstituted vesicles occur, the chl a/b LHC should partition into the areas of membrane contact, similar to the segregation of the large chl a/b LHC-containing E-face particles into the stacked areas of the chloroplast membranes (31, 4). Our investigation has demonstrated that the reconstituted chl a/b LHC membranes possess all of these features. Thus, the chl a/b LHC appears as an ~80-Å particle on the fracture faces of the vesicles, and protruding elements of the particles can be visualized on the vesicle surfaces. The cation concentrations needed to promote adhesion between the reconstituted chl a/b LHC membranes (≥2 mM $MgCl_2$ and ≥60 mM NaCl) are essentially the same as those that produce restacking of experimentally unstacked thylakoids (31, 33). Finally, stacking of the reconstituted membranes leads both to the aggregation of the chl a/b LHC particles in the adhesion zones and to the precise alignment of particles in adjacent membranes, suggesting that the adhesion is mediated by interactions between specific surface exposed sites on the chl a/b LHC particles in adjoining membranes.

This interaction is particularly well illustrated in Fig. 17. In this case, the area of high particle density extends beyond the area of actual membrane contact, presumably because of lateral interactions between chl a/b LHC molecules within the plane of one membrane. However, in the region of actual membrane contact the adhering particles of both membranes exhibit a clear change in their substructure, which is most likely a result

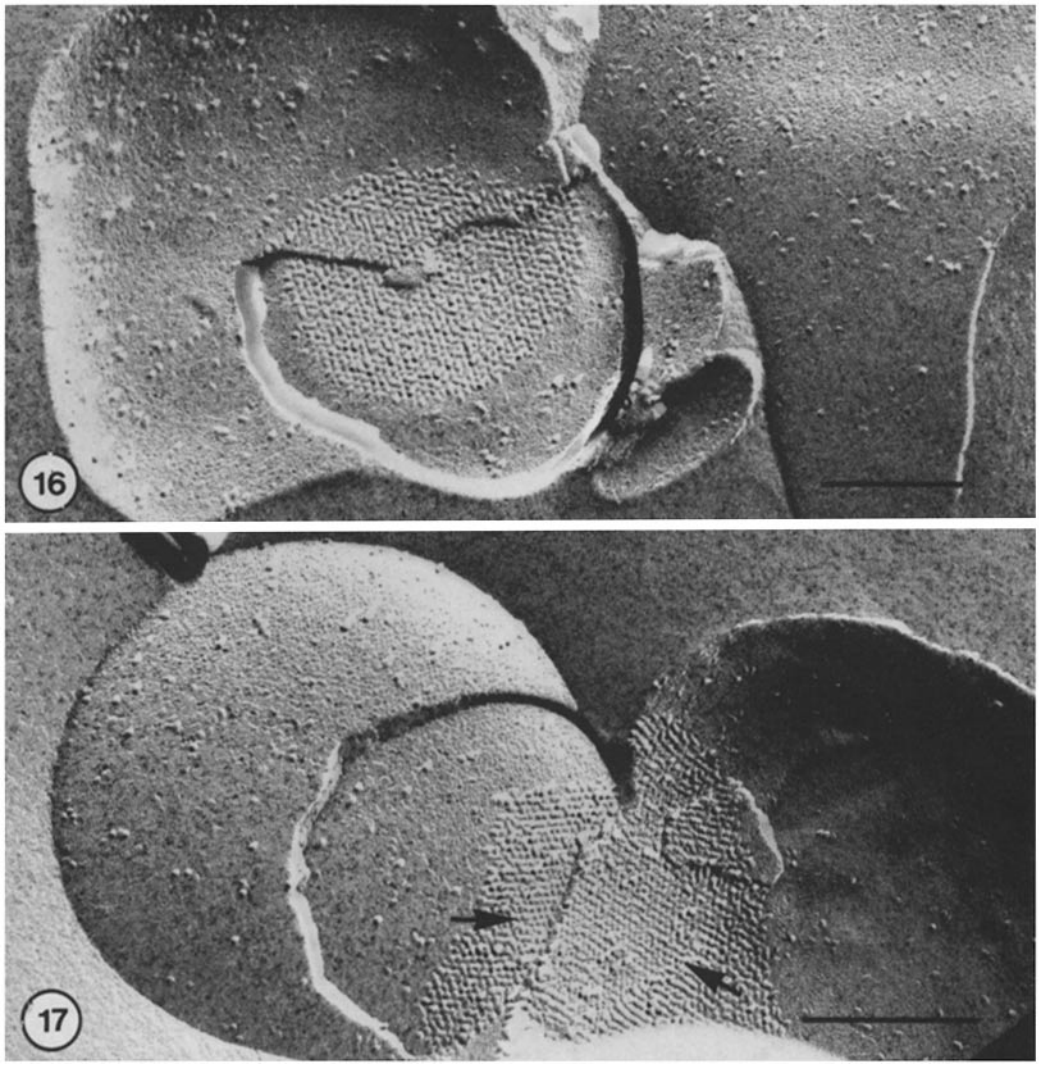

FIGURE 16 Reconstituted lipid vesicles in the presence of 100 mM NaCl. Note the aggregation of the chl a/b LHC particles into a hexagonal array in the area of membrane contact between the vesicles on the left. In the surrounding nonadhering membrane regions, the particles are randomly distributed. × 95,000.

FIGURE 17 Same sample as in Fig. 16. In this case the particle patches exceed the area of membrane contact between the two vesicles. However, the region of actual membrane adhesion is clearly visible due to a subtle change in the organization of the particles within the array of both membranes (arrows). × 117,000.

of the direct interaction of adhering chl a/b LHC particles. This change could reflect a true conformational change of the particles when they link up with each other, or it could be due to the physical stress caused by the Brownian motion of the adjoining vesicles. Another indication as to the nature of the adhesion forces is our finding that adhering, reconstituted chl a/b LHC membranes can fracture along their true surface, i.e., between the adhering chl a/b LHC particles (Fig. 18). This observation provides direct structural support for the hypothesis that the adhesion between chloroplast thylakoids is mediated by hydrophobic interactions (28, 31). In this context, cations are needed

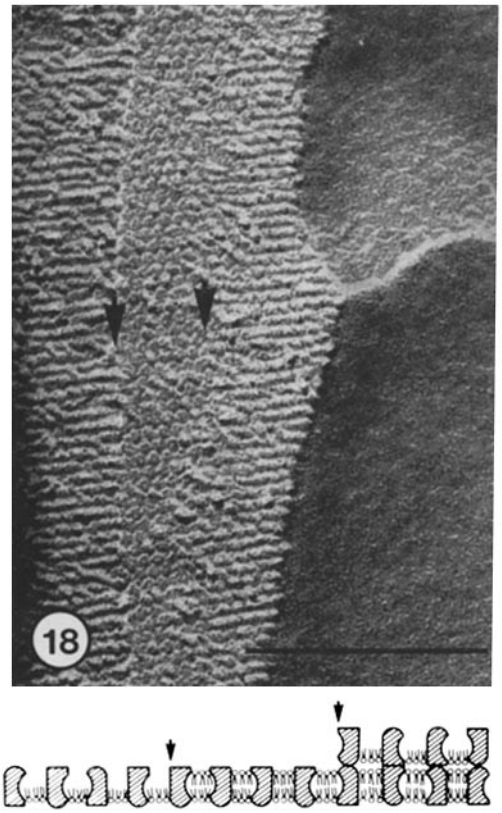

FIGURE 18 Freeze-fracture micrograph of a reconstituted membrane and schematic diagram illustrating the supposed "surface fracture." Corresponding areas in the micrograph and the diagram are marked by arrows. Due to the high density of hydrophobic sites exposed on the membrane surface by the interaction of chl a/b LHC particles, the fracture plane has developed for a short distance over the true membrane surface. In this area the particles appear uniform in size and with a ringlike substructure. × 160,000.

to neutralize the charged groups in the vicinity of the hydrophobic regions (33, 9), which are then able to interact with each other in adjacent membranes. We believe that the charged groups are essential for maintaining the hydrophobic surface groups of the chl a/b LHC in the proper orientation for membrane adhesion, since mild pronase treatment of experimentally unstacked chloroplast membranes, which removes an ~1,000-dalton segment of the chl a/b LHC (13), increases significantly the concentration of cations needed to induce membrane stacking (13) and abolishes the cation-induced precipitation of the solubilized chl a/b LHC from sucrose gradients.

An interpretative summary of the action of cations on the structural organization of the Triton-solubilized and reconstituted chl a/b LHC is diagrammed in Fig. 19.

Electrophoretic Analysis of the LHC

Our finding of a chlorophyll-protein complex, CPII*, with low electrophoretic mobility in Triton-solubilized chl a/b LHC samples of two different plant species provides clear evidence that the chl a/b LHC can exist in an apparent high molecular weight form (2, 7, 19, 21, 22). Both CPII* and CPII show a qualitatively identical polypeptide pattern upon re-electrophoresis with three polypeptides ranging from 25 to 23 kdaltons, and in ratios that differ slightly in different chl a/b LHC samples. A similar polypeptide pattern has also been reported by Bose et al. (11) for the isolated chl a/b LHC of peas (but see reference 16 for a discussion of different findings). To render our gels comparable with those reported in the literature, we have used a variety of solubilization buffers, all resulting in a near-identical polypeptide pattern of the electrophoresed chl a/b LHC. By re-electrophoresis of the excised pigment-protein bands, we have further reduced the likelihood of contaminating comigrating peptides that might unspecifically bind to the chlorophyll-protein complexes. Therefore, we feel that our results on the polypeptide composition of the CPII* and CPII showing three polypeptides associated with them are valid. This, however, leaves that dilemma of how to accommodate three polypeptides with individual mol wt of ~25 kdaltons within the CPII complex which has an apparent mol wt of 30 kdaltons. This question has also been addressed by Henriques and Park (20), who suggest that the broad CPII band represents three individual comigrating chl-binding peptides, rather than a true complex. We proposed here a modification of their interpretation that can account for most of the discrepancies in the data published by different groups. Our hypothesis is that the chl a/b LHC consists of one basic protein, and that this protein is post-translationally modified, i.e., glycosylated (3, 26) or phosphorylated (10) or otherwise altered to allow for the binding of either chl a or b. Alternatively, the chl a/b LHC could consist of two different proteins with similar electrophoretic mobilities and which share common amino acid sequences (14). Approximately equimolar amounts of the chl a and chl b binding

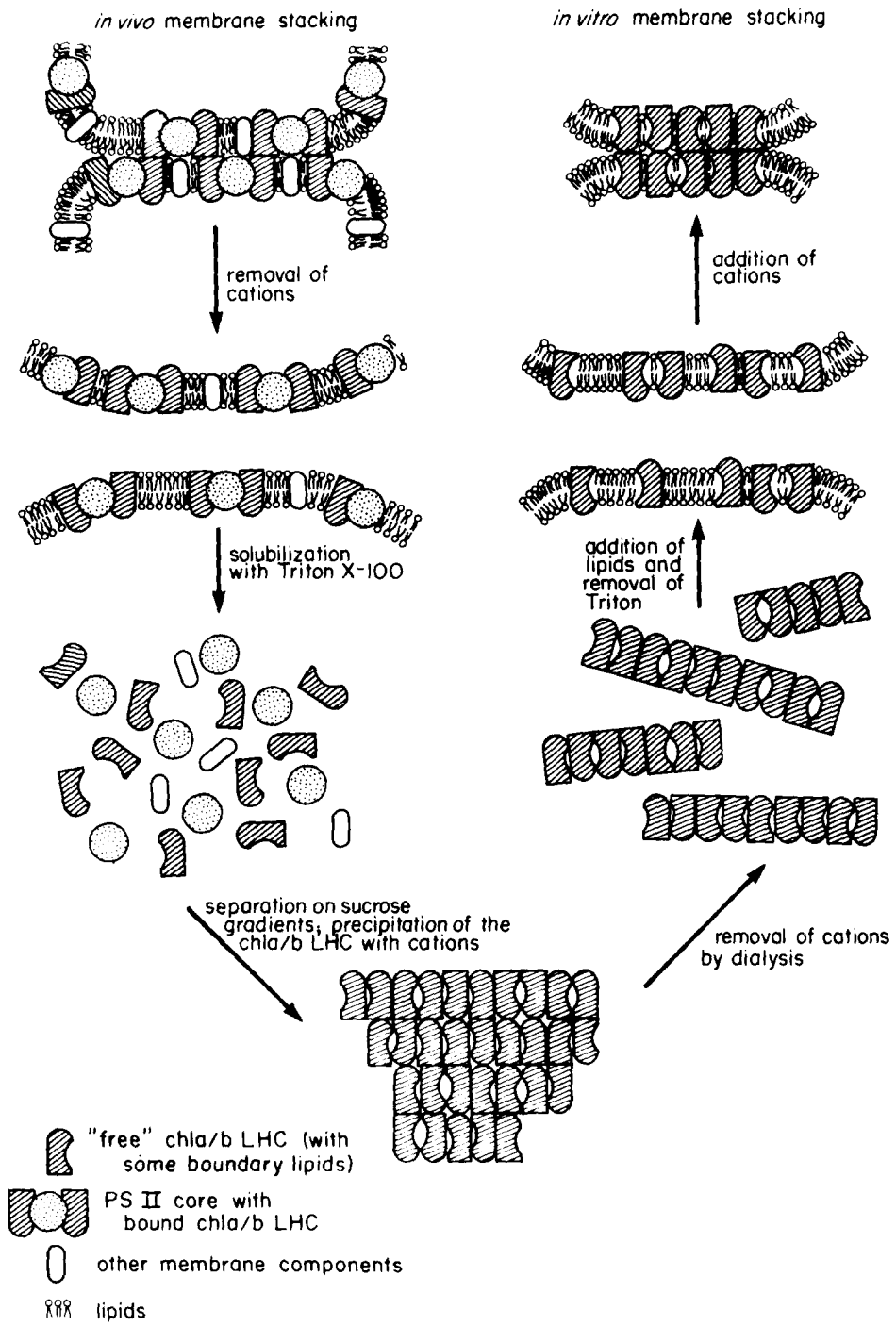

FIGURE 19 Diagram summarizing the isolation and purification of the chl a/b LHC from chloroplast membranes, its reconstitution into lipid vesicles, and the chl a/b LHC-mediated membrane-membrane interaction of the reconstituted vesicles in the presence of cations. The chl a/b LHC is drawn as spanning the membrane based on the analysis of deep-etched thylakoid membrane (31) and on accessibility of the chl a/b to pronase (13). Note that upon addition of cations the Triton-solubilized chl a/b LHC form paracrystalline aggregates which break up into membranous sheets when cations are removed by dialysis. After solubilization with Triton and addition of external lipids, remnants of these membranous sheets frequently remain as particle patches beside the randomly distributed particles in the reconstituted vesicles. Re-addition of cations leads to adhesion of the reconstituted membranes due to cation-mediated interactions between particles of adjacent membranes, which become concentrated in the area of membrane contact.

proteins aggregate to form the in vivo chl a/b LHC complex. Under mild solubilization conditions, this complex can be partially preserved and migrates as a high molecular weight complex CPII* on polyacrylamide gels. Under harsher conditions, however, the complex first dissociates into stable subgroups of chl-binding peptides (25), giving rise to the conspicuously broad green band of CPII and, ultimately, three peptides that have lost their chlorophylls and are separated due to their slightly different side groups or other modifications. Consequently, we do not consider CPII* a dimer or oligomer of CPII, but rather a true equivalent of the native chl a/b LHC and most similar to the Triton-solubilized chl a/b LHC, both of which may have a mol wt of ~200,000 daltons (see first section of the Discussion). CPII, on the other hand, would represent a mixture of semistable dissociation products.

Taken together, our results indicate that the chl a/b LHC plays a dual role in chloroplast membranes. Besides serving as the main light-harvesting antenna (35), it also is responsible for the adhesion of chloroplast membranes in grana stacks. Since our preparation of the Triton chl a/b LHC is comprised of a small number of peptides, the stage appears set for the characterization of the molecular basis of membrane-membrane interaction in chloroplasts.

The functional significance of membrane stacking in chloroplasts is still not completely understood. However, since membrane stacking is observed in all higher plants and green algae and has also been recently observed in the chl b containing prokaryote, *Prochloron*,[1] it seems to be a very ancient feature of thylakoid membranes, presumably endowing carriers of this feature with a selective advantage. In this context, stacking would not only allow for a more efficient packing of the photosynthetic membranes, but might also provide simultaneously a mechanism by which the components of the photosynthetic electron chain become concentrated in the stacked regions. This concentration of the electron-chain components could increase the efficiency of photosynthesis under low-light conditions.

[1] Giddings, T. H., and L. A. Staehelin. Supramolecular structure of stacked and unstacked regions of the photosynthetic membranes of *Prochloron* sp., a prokaryote. Manuscript submitted for publication.

The authors gratefully acknowledge the expert technical assistance of Marcia DeWit and the helpful discussions with Dr. Winfried Boos and Susan Spath.

Supported by grants GM 18639 and GM 22912.

Received for publication 11 June 1979, and in revised form 24 September 1979.

REFERENCES

1. ANDERSON, J. M. 1975. The molecular organization of chloroplast thylakoids. *Biochim. Biophys. Acta* **416**:191–235.
2. ANDERSON, J. M., J. C. WALDRON, and S. W. THORNE. 1978. Chlorophyll-protein complexes of spinach and barley thylakoids. *FEBS (Fed. Eur. Biochem. Soc.) Lett.* **92**:227–233.
3. APEL, K. 1977. The light-harvesting chlorophyll a/b protein complex of the green alga *Acetabularia mediterranea*. Isolation and characterization of two subunits. *Biochim. Biophys. Acta* **462**:390–402.
4. ARMOND, P. A., L. A. STAEHELIN, and C. J. ARNTZEN. 1977. Spatial relationships of photosystem I, photosystem II, and the light harvesting complex in chloroplast membranes. *J. Cell Biol.* **73**:400–418.
5. ARNTZEN, C. J. 1978. Dynamic structural features of chloroplast lamellae. *Curr. Top. Bioenerg.* **8**:111–160.
6. ARNTZEN, C. J., and C. L. DITTO. 1976. Effects of cations upon chloroplast membrane subunit interactions and excitation energy distribution. *Biochim. Biophys. Acta* **449**:259–274.
7. ARO, E.-M., and N. VALANNE. 1978. Effect of magnesium on chlorophyll-protein complexes. *Physiol. Plant.* **43**:261–264.
8. BARBER, J. 1976. Ionic regulation of intact chloroplasts and its effect on primary photosynthetic processes. *In* The Intact Chloroplast. J. Barber, editor, Elsevier/North Holland Biomedical Press, Amsterdam. 89–134.
9. BARBER, J. 1979. Energy transfer and its dependence on membrane properties. *Ciba Found. Symp.* **61**: 283–304.
10. BENNETT, J. 1977. Phosphorylation of chloroplast membrane polypeptides. *Nature (Lond.).* **269**:344–346.
11. BOSE, S., J. J. BURKE, and C. J. ARNTZEN. 1977. Cation induced microstructural changes in chloroplast membranes: Effects on photosystem II activity. *In* Bioenergetics of Membranes. L. Packer, editor. Elsevier/North Holland Biomedical Press, Amsterdam. 245–256.
12. BURKE, J. J., C. L. DITTO, and C. J. ARNTZEN. 1978. Involvement of the light-harvesting complex in cation regulation of excitation energy distribution in chloroplasts. *Arch. Biochem. Biophys.* **187**:252–263.
13. CARTER, D. P., and L. A. STAEHELIN. 1979. *Arch. Biochem. Biophys.* In press.
14. CHUA, N.-H., and F. BLOMBERG. 1979. Immunochemical studies of thylakoid membrane polypeptides from spinach and *Chlamydomonas reinhardtii*. A modified procedure for crossed immunoelectrophoresis of dodecyl sulfate-protein complexes. *J. Biol. Chem.* **254**:215–223.
15. DELEPELAIRE, P., and N.-H. CHUA. 1979. Lithium dodecyl sulfate/polyacrylamide gel electrophoresis of thylakoid membranes at 4°C: Characterization of two additional chlorophyll a-protein complexes. *Proc. Natl. Acad. Sci. U. S. A.* **76**:111–115.
16. DUNKLEY, P. R., and J. M. ANDERSON. 1979. The light harvesting chlorophyll a/b protein complex from barley thylakoid membranes. Polypeptide composition and characterization of an oligomer. *Biochim. Biophys. Acta* **545**:174–187.
17. GERRITSEN, W. J., A. J. VERKLEIJ, R. F. A. ZWAAL, and L. L. M. VAN DEENEN. 1978. Freeze-fracture appearance and disposition of band 3 protein from the human erythrocyte membrane in lipid vesicles. *Eur. J. Biochem.* **85**:255–261.
18. GREEN, D. E., and S. FLEISCHER. 1963. The role of lipids in mitochondrial electron transfer and oxidative phosphorylation. *Biochim. Biophys. Acta.* **70**:554–582.
19. HAYDEN, D. B., and W. J. HOPKINS. 1976. Membrane polypeptides and chlorophyll-protein complexes of maize and mesophyll chloroplasts. *Can. J. Bot.* **54**:1684–1689.
20. HENRIQUES, F., and R. PARK. 1977. Polypeptide composition of chlorophyll protein complexes from Romaine lettuce. *Plant Physiol.* **60**:64–68.
21. HENRIQUES, F., and R. PARK. 1978. Characterization of three new chlorophyll protein complexes. *Biochem. Biophys. Res. Commun.* **81**: 1113–1118.
22. HILLER, R. G., T. B. G. PILGER, and D. CAMPBELL. 1979. Extraction and stabilization of the dimer of chlorophyll-protein complex II. *Plant Sci. Lett.* **14**:7–11.
23. IZAWA, S., and N. E. GOOD. 1966. Effects of salts and electron transport on the conformation of isolated chloroplasts. II. Electron Microscopy. *Plant Physiol.* **14**:544–552.

24. LAEMMLI, U. K. 1970. Cleavage of structural proteins during the assembly of the head of bacteriophage T4. *Nature (Lond.)*. **227**:680–685.
25. MACHOLD, O., and A. MEISTER. 1979. Resolution of the light harvesting chlorophyll a/b protein of *Vicia faba* chloroplasts into two different chlorophyll-protein complexes. *Biochim. Biophys. Acta.* **546**:472–480.
26. MCDONNEL, A., D. P. CARTER, and L. A. STAEHELIN. 1977. Chloroplast membrane proteins: Detection of hemoproteins and glycoproteins on polyacrylamide gels. *J. Cell Biol.* **75** (2, Pt. 2): 224 *a*. (Abstr.).
27. MILLER, K. R., and L. A. STAEHELIN. 1976. Analysis of the thylakoid outer surface. Coupling factor is limited to unstacked membrane regions. *J. Cell Biol.* **68**:30–47.
28. MURAKAMI, S., and L. PACKER. 1971. The role of cations in the organization of chloroplast membranes. *Arch. Biochem. Biophys.* **146**: 337–347.
29. OJAKIAN, G. K., and P. SATIR. Particle movements in chloroplast membranes: Quantitative measurements of membrane fluidity by the freeze-fracture technique. *Proc. Natl. Acad. Sci. U. S. A.* **71**:2052–2056.
30. PROCHASKA, L. J., and E. L. GROSS. 1977. Evidence for the location of divalent cation binding sites of the chloroplast membrane. *J. Membr. Biol.* **36**:13–32.
31. STAEHELIN, L. A. 1976. Reversible particle movements associated with unstacking and restacking of chloroplast membranes *in vitro*. *J. Cell Biol.* **71**:136–158.
32. STAEHELIN, L. A., P. A. ARMOND, and K. R. MILLER. 1977. Chloroplast membrane organization on the supramolecular level and its functional implication. *Brookhaven Symp. Biol.* **28**:278–315.
33. STAEHELIN, L. A., and C. J. ARNTZEN. 1979. Effects on ions and gravity forces on the supramolecular organization and excitation energy distribution in chloroplast membranes. *Ciba Found. Symp.* **61**:147–175.
34. TAKAHASHI, M., and E. L. GROSS. 1978. Use of immobilized light-harvesting chlorophyll a/b protein to study the stoichiometry of its self-association. *Biochemistry.* **17**:806–810.
35. THORNBER, J. P. 1975. Chlorophyll-proteins: Light-harvesting and reaction center components of plants. *Annu. Rev. Plant Physiol.* **26**:127–158.